ISSN: 1410-8917
Jurnal Kimia Sains & Aplikasi
e-ISSN: 2597-9914

Jurnal Kimia Sains dan Aplikasi 29 (7) (2026): 476-490

Jurnal Kimia Sains dan Aplikasi
Journal of Scientific and Applied Chemistry

Journal homepage: http://ejournal.undip.ac.id/index.php/ksa

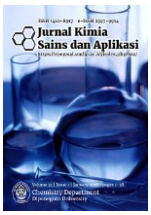

Low-Cost Rice Husk Ash-Based Adsorbent for Surfactant and Phosphate Removal from Laundry Wastewater

Julinawati [1,*], Faradilla [1], Irfan Mustafa [1], Suryati [2], Andriy Anta Kacaribu [3]

[1] Department of Chemistry, Faculty of Mathematics and Natural Sciences, Universitas Syiah Kuala, Banda Aceh 23111, Indonesia
[2] Department of Chemical Engineering, Universitas Malikussaleh, Lhokseumawe 24351, Indonesia
[3] Doctoral of Agricultural Science, Postgraduate School Universitas Syiah Kuala, Banda Aceh 23111, Indonesia

* Corresponding author: julinawati@usk.ac.id

https://doi.org/10.14710/jksa.29.7.476-490

Article Info

Article history:

Received: 24th May 2026
Revised: 12th July 2026
Accepted: 17th July 2026
Online: 31st August 2026

Keywords:
Rice husk ash; Acid activation; Laundry wastewater; Surfactant removal; Phosphate removal; Adsorption

Abstract

The discharge of laundry wastewater containing surfactants and phosphates represents a growing environmental concern, particularly in areas where wastewater is released without adequate treatment. This study evaluates sulfuric acid–activated rice husk ash (RHA) as a low-cost adsorbent for removing surfactants and phosphates from real laundry wastewater. FTIR and XRD analyses indicated that the main silica-related functional groups and framework of RHA were largely retained after acid activation, while SEM observations suggested a rougher and more heterogeneous surface morphology. Batch adsorption experiments using real laundry wastewater showed that surfactant and phosphate removal were influenced by adsorbent dosage and contact time. The optimum dosage was 3 g for surfactant removal and 4 g for phosphate removal, while the optimum contact time for both contaminants was 30 min. Controlled isotherm experiments using separate single-solute surfactant and phosphate standard solutions indicated that the adsorption behavior of both contaminants was better described by the Freundlich model, suggesting adsorption on heterogeneous surface sites. Kinetic analysis using real laundry wastewater showed rapid uptake, with the Elovich model providing the best overall fit for both surfactant and phosphate adsorption. These findings suggest that sulfuric acid–activated RHA is a promising, simple, and affordable biomass-derived adsorbent for laundry wastewater treatment, although further studies involving surface area analysis, regeneration, reusability, column operation, and cost performance are required to support practical application.

1. Introduction

The rapid growth of laundry services has led to an increase in wastewater generation, which is often discharged directly into drainage systems without adequate treatment [1, 2]. Laundry wastewater commonly contains surfactants and phosphates originating from detergent formulations, and these contaminants can negatively affect aquatic environments when released untreated [3, 4]. Surfactants, particularly anionic surfactants, can reduce surface tension, generate persistent foam, and interfere with oxygen transfer in aquatic systems [5, 6, 7]. Phosphates act as nutrients that promote eutrophication, leading to excessive algal growth and oxygen depletion in receiving water bodies [8, 9]. Therefore, the removal of both surfactants and phosphates is important for improving the quality of laundry wastewater before discharge.

Various treatment methods have been applied for laundry wastewater treatment, including coagulation–flocculation [10, 11], advanced oxidation processes [12, 13], membrane filtration [14], biological treatment [15], and adsorption [16]. Among these methods, adsorption is attractive because of its operational simplicity, relatively low energy requirement, and adaptability to different pollutant types [17]. Conventional adsorbents such as activated carbon and zeolite have been widely used;

however, their cost and regeneration requirements may limit their application in small-scale or decentralized treatment systems [16, 18]. For this reason, low-cost biomass-derived adsorbents have gained increasing attention as alternative materials for wastewater treatment [19, 20, 21, 22].

Rice husk ash (RHA) is an abundant agricultural by-product in rice-producing countries and is rich in silica-based components that can contribute to adsorption processes [23, 24, 25]. The silica-rich surface of RHA contains silanol (Si–OH) and siloxane (Si–O–Si) groups, which can provide interaction sites for polar contaminants through hydrogen bonding, electrostatic interactions, and weak surface complexation [26]. These surface groups are relevant for surfactant and phosphate adsorption because surfactant molecules can interact through their polar head groups and hydrophobic moieties, while phosphate ions can interact with hydroxyl-containing sites on the silica surface.

Previous studies have reported the use of rice husk- and RHA-based materials for wastewater treatment. Dadebo *et al.* [11] applied rice husk ash as a coagulant followed by activated carbon adsorption for surfactant-laden wastewater treatment, but the process required sequential treatment steps and more than one treatment material. Other work reported by Hosseinnia *et al.* [27] also showed that rice husk could act as a low-cost adsorbent for surfactant removal from wastewater, indicating the potential of rice husk-based materials for detergent-related pollutants. For phosphate removal, Lugo-Arias *et al.* [23] reported the use of rice husk-derived adsorbents, including Mg-modified rice husk bioadsorbents, for nitrate and phosphate removal from aqueous solutions. However, their work was conducted mainly in synthetic aqueous systems rather than in real laundry wastewater, and the improved phosphate uptake was attributed to mineral modification.

Chemically modified RHA and rice husk-derived silica have also been developed to enhance adsorption performance, particularly for anionic pollutants. Phan *et al.* [28] prepared amine-functionalized activated RHA for the simultaneous removal of organic pollutants, nitrate, and phosphate in wastewater, demonstrating that amine functionalization can improve multi-pollutant adsorption capacity. Similarly, Suzaimi *et al.* [29] developed branched polyethyleneimine-grafted porous rice husk silica for phosphate adsorption, where phosphate uptake was enhanced by protonated amine groups, electrostatic attraction, ion exchange, hydrogen bonding, and possible inner-sphere complexation. These studies confirm the potential of chemically modified RHA or rice husk-derived silica for anion adsorption; however, they generally involve more advanced functionalization routes or focus on synthetic/controlled aqueous systems.

Sulfuric acid activation was selected in the present study as a simpler chemical treatment because acid leaching can remove soluble inorganic impurities and partially clean the ash surface, thereby exposing silica-related functional groups such as silanol and siloxane groups. Acid treatment can also reduce ash-associated mineral residues that may block surface sites, increase the relative accessibility of the silica-rich matrix, and promote hydroxyl-related surface features relevant to adsorption. Compared with untreated RHA, acid-activated RHA is expected to provide a cleaner, more accessible surface for pollutant interactions, while remaining less complex than amine-functionalized, metal-modified, or polymer-grafted adsorbents.

Despite these developments, the use of simply prepared sulfuric acid–activated RHA as a single-step, waste-derived adsorbent for removing surfactants and phosphates from real laundry wastewater remains insufficiently explored. Unlike amine-functionalized or metal-modified RHA-based adsorbents, the present study evaluates a simpler acid-activation approach using RHA directly as a low-cost adsorbent. This approach was chosen to balance surface improvement, material availability, and preparation simplicity for potential decentralized wastewater treatment applications. The adsorption performance was assessed through dosage and contact time experiments using real laundry wastewater, while controlled isotherm experiments using separate standard solutions were conducted to provide supporting insight into the individual adsorption behavior of surfactants and phosphate. This work is intended to distinguish the practical applicability of acid-activated RHA from more complex or highly engineered adsorbent systems for decentralized laundry wastewater treatment.

2. Experimental

2.1. Materials

Rice husk ash was used as the adsorbent precursor. Real laundry wastewater was collected as the adsorbate source. Sulfuric acid (H_2SO_4), sodium hydroxide (NaOH, 1 N), standard linear alkyl sulfonate (LAS), phenolphthalein indicator (0.5% w/v), methylene blue, chloroform ($CHCl_3$), sodium dihydrogen phosphate monohydrate ($NaH_2PO_4.H_2O$), potassium dihydrogen phosphate (KH_2PO_4), isopropanol (i-C_3H_7OH), potassium antimony tartrate [$K(SbO)C_4H_4O_6{\cdot}1/2H_2O$], ammonium molybdate [$(NH_4)_6Mo_7O_{24}{\cdot}4H_2O$], and ascorbic acid ($C_6H_8O_6$, 0.1 M) were of analytical grade, purchased from Merck and Sigma-Aldrich (Malaysia), and used without further purification. Deionized water was used throughout the experiments.

2.2. Adsorbent Feedstock Preparation and Wastewater Sampling

RHA was obtained from the open combustion of rice husk residues collected from agricultural fields in Jangka Alue Village, Bireuen Regency, Indonesia. The RHA was transported to the laboratory and manually cleaned to remove impurities, including residual wood fragments, stones, and other foreign materials. The cleaned ash was washed several times with deionized water to remove adhering dust and soluble impurities, then oven-dried at 105°C until a constant weight was achieved.

Real laundry wastewater was collected from a commercial laundry facility located in Lueng Bata District, Banda Aceh, Indonesia. Grab sampling was

conducted following standard wastewater sampling procedures [30]. The samples were collected in clean polyethylene containers, transported to the laboratory in an icebox, and stored at 4°C prior to analysis. The initial pH of the raw laundry wastewater was 8.1. No pH adjustment was performed before the adsorption experiments to preserve the original wastewater matrix and to evaluate the performance of acid-activated RHA under practical treatment conditions.

2.3. Acid Activation of Rice Husk Ash

Chemical activation of RHA was performed using 1 M H_2SO_4. The dried ash was ground in a ball mill for 30 minutes and sieved to obtain particles of 100 mesh. Subsequently, 50 g of the sieved ash was immersed in 200 mL of 1 M H_2SO_4 and soaked for 24 h at room temperature. The mixture was then filtered, and the residue was washed repeatedly with deionized water until the filtrate reached neutral pH. The activated ash was oven-dried at 200°C for 2 h and stored in a desiccator for further use. The physicochemical characteristics of the adsorbent before and after activation were analyzed using Fourier transform infrared spectroscopy (FTIR, Shimadzu Japan), X-ray diffraction (XRD PANalytical X'pert PRO instrument, at 2θ = 15–40° and scanning electron microscopy (SEM, JEOL JSM-6390 LA).

2.4. Determination of Surfactant and Phosphate Concentrations in Laundry Wastewater

The concentrations of surfactant and phosphate in real laundry wastewater were determined using UV–Vis spectrophotometric methods in accordance with the standard of examination for water and wastewater [30]. The measured concentrations were used as baseline values to evaluate adsorption performance before and after treatment.

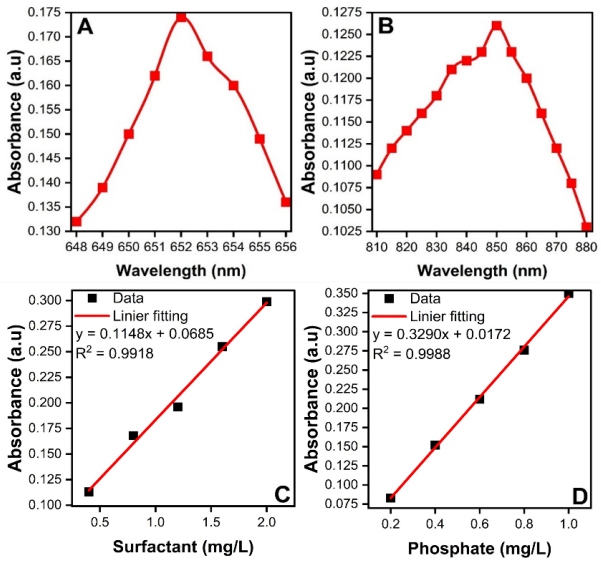

Figure 1. Determination of the maximum absorption wavelength (λ_{max}) of (A) surfactant and (B) phosphate, and the corresponding calibration curves for (C) surfactant and (D) phosphate obtained using UV–Vis spectrophotometry

Surfactant concentration was quantified using the methylene blue active substances (MBAS) method, which is based on the formation of a blue-colored ion-pair complex between anionic surfactants and methylene blue that is extractable into an organic solvent [4]. Standard solutions were prepared from LAS with concentrations ranging from 0.4 to 2.0 mg/L. The maximum absorption wavelength (λ_{max}) was determined by scanning a representative standard solution in the range of 600–680 nm (Figure 1A). The absorbance of the extracted organic phase was measured at 652 nm, and a calibration curve was constructed using the standard solutions (Figure 1C). Laundry wastewater samples were analyzed in duplicate following the same procedure, and surfactant concentrations were calculated from the calibration curve. The initial surfactant concentration in the wastewater was 7.82 mg/L.

Phosphate concentration was determined using the ascorbic acid–molybdenum blue spectrophotometric method [4]. In this method, orthophosphate reacts with ammonium molybdate and potassium antimony tartrate under acidic conditions to form phosphomolybdic acid, which is subsequently reduced by ascorbic acid to produce a blue molybdenum complex. Phosphate standard solutions in the range of 0.2–1.0 mg/L were used to construct the calibration curve. The λ_{max} was determined by scanning a representative standard solution in the range of 810–880 nm (Figure 1B), and absorbance was measured within 10–30 min after reagent addition. The calibration curve is shown in Figure 1D. Laundry wastewater samples were analyzed in duplicate under identical conditions. The initial phosphate concentration in the wastewater was 0.73 mg/L.

2.5. Batch Adsorption Experiments

2.5.1. Effect of Adsorbent Dosage

Batch adsorption experiments were conducted by adding 1, 2, 3, 4, 5, and 6 g of activated RHA into 120 mL of laundry wastewater in Erlenmeyer flasks. The mixtures were agitated at 200 rpm for 30 min at room temperature. All batch adsorption experiments using real laundry wastewater were conducted without pH adjustment. This approach was selected to simulate practical decentralized wastewater treatment conditions and to avoid additional chemical input during treatment. Although pH is an important parameter for silica-based adsorbents, pH optimization was beyond the scope of the present study and should be evaluated in future work. After filtration, the residual concentrations of surfactant and phosphate were analyzed.

2.5.2. Effect of Contact Time

Adsorption experiments were carried out using the optimum adsorbent dosage with contact times of 15, 30, 45, and 60 min under identical agitation conditions. After adsorption, the spent adsorbent under optimal conditions was characterized by FTIR to evaluate changes in functional groups.

2.6. Adsorption Isotherm and Kinetics Analysis

Adsorption isotherm experiments were conducted separately for surfactant and phosphate using single-solute standard solutions with different initial concentrations. Surfactant standard solutions were prepared from LAS, whereas phosphate standard solutions were prepared from potassium dihydrogen phosphate. The surfactant and phosphate standard solutions were not mixed during the isotherm experiments. Therefore, the isotherm analysis was used to evaluate the intrinsic equilibrium adsorption behavior of each contaminant on acid-activated RHA, rather than the simultaneous adsorption behavior in real laundry wastewater. This controlled approach was used to minimize matrix interference from real laundry wastewater and to allow systematic variation of the initial concentration (C_0) required for Langmuir and Freundlich model fitting. Thus, the isotherm experiments complement the batch adsorption studies by providing supporting information on the individual equilibrium adsorption tendency of surfactant and phosphate under controlled conditions.

A fixed mass of acid-activated RHA was added to 120 mL of each standard solution and agitated at 200 rpm for 30 min at room temperature. After adsorption, the suspensions were filtered, and the residual surfactant and phosphate concentrations were determined using UV–Vis spectrophotometry. The equilibrium adsorption capacity, q_e, was calculated using Equation 1.

$$q_e = \frac{(C_0 - C_e)V}{m} \quad (1)$$

where q_e is the adsorption capacity at equilibrium (mg/g), C_0 is the initial adsorbate concentration (mg/L), C_e is the equilibrium adsorbate concentration (mg/L), V is the solution volume (L), and m is the mass of adsorbent (g).

The equilibrium data were fitted using the linear forms of the Langmuir and the Freundlich isotherm models. The linearized Langmuir and Freundlich equations are presented in Equations 2 and 3, respectively.

$$\frac{C_e}{q_e} = \frac{1}{K_L q_{max}} + \frac{C_e}{q_{max}} \quad (2)$$

$$Log\ q_e = \log K_F + \frac{1}{n}\log C_e \quad (3)$$

where q_e (mg/g) is the adsorption capacity at equilibrium, C_e (mg/L) is the equilibrium concentration of the adsorbate; q_{max} (mg/g) is the maximum adsorption capacity, K_L (L/mg) is the Langmuir adsorption constant related to the affinity between adsorbate and adsorbent, K_F ((mg/g)(L/mg)$^{1/n}$) is the Freundlich adsorption constant; and n is the adsorption intensity parameter.

In contrast to the isotherm experiments, adsorption kinetic experiments were conducted using real laundry wastewater to evaluate the time-dependent removal behavior under realistic wastewater conditions. The kinetic experiments were performed using the optimum adsorbent dosage, a solution volume of 120 mL, an agitation speed of 200 rpm, and different contact times at room temperature. After each contact time, the suspension was filtered, and the residual surfactant and phosphate concentrations were measured using UV–Vis spectrophotometry. The adsorption capacity at time t, q_t, was calculated using Equation 4.

$$q_t = \frac{(C_0 - C_t)V}{m} \quad (4)$$

where q_t is the adsorption capacity at time t (mg/g), and C_t is the adsorbate concentration at time t (mg/L).

To describe the kinetic adsorption behavior, the experimental data were fitted using commonly applied non-linear kinetic models, including the pseudo-first-order, pseudo-second-order, and Elovich models. The non-linear forms of the kinetic equations were applied to avoid potential bias associated with linearization.

3. Results and Discussion

3.1. Characterization of RHA-based Adsorbent

Figure 2 presents the visual appearance, FTIR spectra, XRD patterns, and SEM images of the RHA adsorbent before and after sulfuric acid activation. A visible color change from grayish to slightly yellowish-white was observed after acid activation (Figure 2A–B). This change suggests the partial removal of impurities and modification of the surface composition during acid treatment. Acid leaching can dissolve soluble inorganic components and residual contaminants, thereby producing a cleaner silica-rich surface [31]. This provides a rationale for using sulfuric acid activation, as the removal of soluble impurities and partially blocking mineral residues can improve the observable surface cleanliness, expose silica-related functional groups, and increase the apparent accessibility of the RHA surface.

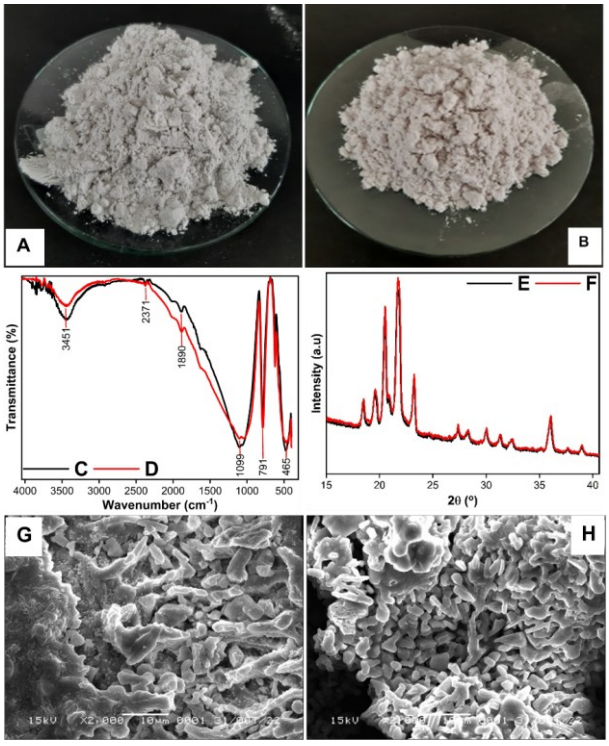

Figure 2. Visual appearance, FTIR spectra, XRD patterns, and SEM images of the prepared RHA adsorbent before activation (A, C, E, G) and after sulfuric acid activation (B, D, F, H)

The FTIR spectra of RHA before and after activation are shown in Figure 2C–D. Both spectra exhibit characteristic absorption bands associated with silica-based materials, particularly Si–O–Si and Si–O stretching vibrations, indicating that siloxane-related groups dominate the surface chemistry of the adsorbent [32]. The absence of major peak shifts after activation suggests that the main silica framework of RHA was largely preserved during sulfuric acid treatment.

However, the broad absorption band around 3451 cm^{-1}, corresponding to –OH stretching vibrations of silanol groups and adsorbed water, became slightly broader after activation. This observation indicates an increased contribution of surface hydroxyl-related groups, which may be associated with surface protonation and hydroxylation during acid treatment [33]. The presence of these hydroxyl-related groups is important because they may provide potential surface sites for interactions with polar adsorbates, including surfactant molecules and phosphate ions. However, the specific interaction pathways cannot be distinguished solely from FTIR, XRD, and SEM analyses. The specific contribution of individual interaction mechanisms requires further confirmation using surface-sensitive analyses such as zeta potential, pH_{pzc}, or XPS.

The phase characteristics of the RHA adsorbent were examined by XRD analysis (Figure 2E–F). The XRD patterns before and after sulfuric acid activation showed broadly similar diffraction profiles, indicating that acid treatment did not cause major structural changes in the silica-based ash matrix. Several diffraction features were observed around 20.53°, 21.76°, and 23.21° before activation and around 20.57°, 21.80°, and 23.25° after activation. These peaks may be associated with silica-related ordered domains, including tridymite- or cristobalite-like phases, although RHA is generally known to be dominated by amorphous silica depending on the combustion conditions [31, 34]. Therefore, the peaks observed in this study should be interpreted with caution as indications of minor ordered silica domains rather than as evidence that the RHA matrix is predominantly crystalline.

SEM images further reveal morphological changes induced by sulfuric acid activation (Figure 2G–H). Before activation, the RHA surface appeared relatively compact, irregular, and partially covered by impurities or agglomerated particles (Figure 2G). After activation, the surface became rougher and more heterogeneous, with visible cavities and channels (Figure 2H). These morphological changes suggest that acid treatment removed some surface impurities and exposed previously blocked surface regions [35]. Although quantitative surface area analysis was not performed, SEM observations indicate that sulfuric acid activation improved the surface accessibility of RHA, potentially facilitating contact between the adsorbent and target pollutants during adsorption.

Overall, the characterization results suggest that sulfuric acid activation modified the observable physicochemical characteristics of RHA without causing major disruption to its silica-based matrix. FTIR analysis indicates the presence of hydroxyl- and siloxane-related functional groups, XRD suggests that the main silica-related phase profile was largely retained after acid activation, and SEM reveals a rougher and more open surface morphology. These combined observations support the potential use of acid-activated RHA as a low-cost adsorbent for removing surfactants and phosphates from laundry wastewater.

3.2. Effect of Adsorbent Dosage

The effect of adsorbent dosage on surfactant and phosphate removal from real laundry wastewater is shown in Figure 3A–B. Adsorbent dosage is an important operational parameter because it determines the number of available surface sites and the adsorbate-to-adsorbent ratio during batch adsorption. The adsorption experiments were conducted without pH adjustment at the initial wastewater pH of 8.1 to represent practical treatment conditions. This pH condition may influence both pollutant speciation and the surface behavior of acid-activated RHA. At a slightly alkaline pH, phosphate is expected to occur mainly as deprotonated species, particularly HPO_4^{2-}, with a smaller contribution from $H_2PO_4^-$. These anionic species may have limited affinity for the negatively charged silica-rich surface because silanol groups become increasingly deprotonated under alkaline conditions. This may partly explain the moderate phosphate removal observed in this study.

In the case of surfactants, anionic surfactants such as LAS are expected to remain negatively charged at wastewater pH, and their adsorption may therefore depend not only on direct surface interactions but also on hydrophobic association, matrix effects, and possible cation bridging or competition with other wastewater constituents. Since zeta potential and pH_{pzc} analyses were not performed, the specific role of surface charge could not be confirmed in this study. Therefore, the pH-related interpretation is presented as a possible explanation for the observed adsorption behavior rather than as definitive mechanistic evidence [36, 37, 38].

For surfactant adsorption (Figure 3A), the removal efficiency increased from 79.73% to 85.91% as the adsorbent dosage increased from 1 to 3 g. This improvement can be attributed to the greater availability of adsorption sites and increased contact area between acid-activated RHA and surfactant molecules. However, increasing the adsorbent dosage further to 4 and 5 g decreased the removal efficiency to 82.96% and 74.94%, respectively. This decline may be associated with particle aggregation, active-site overlap, and reduced effective surface area at higher adsorbent loadings. Excessive adsorbent dosage may also cause interparticle interference and reduce mass-transfer effectiveness, resulting in lower apparent removal efficiency. Similar behavior has been reported in batch adsorption systems [39, 40, 41, 42, 43].

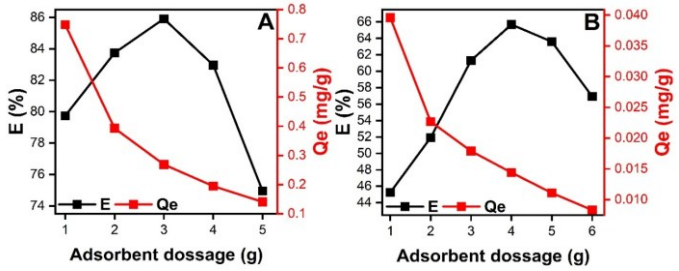

Figure 3. Effect of adsorbent dosage of (A) surfactant and (B) phosphate onto acid-activated RHA. Experimental conditions: solution volume = 0.12 L, temperature = 25°C, agitation speed = 200 rpm, using real laundry wastewater without pH adjustment (initial pH = 8.1)

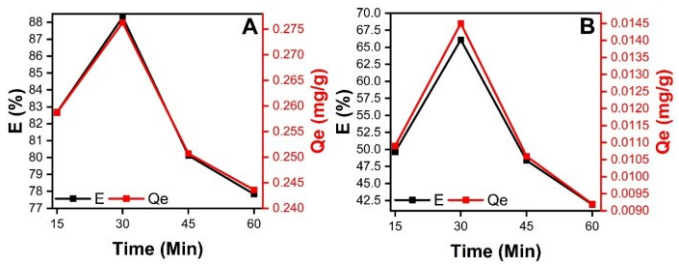

Figure 4. Effect of contact time on the adsorption of (A) surfactant and (B) phosphate onto acid-activated RHA. Experimental conditions: solution volume = 0.12 L, temperature = 25°C, agitation speed = 200 rpm, and using real laundry wastewater without pH adjustment (initial pH = 8.1)

The adsorption capacity, q_e, showed an opposite trend to the removal efficiency. As shown in Figure 3A, q_e decreased continuously from 0.74 mg/g at 1 g to 0.14 mg/g at 5 g. This decrease is expected because the same amount of adsorbate is distributed over a larger mass of adsorbent, resulting in lower adsorbate loading per unit mass of RHA. Therefore, the decrease in q_e at higher adsorbent dosages does not necessarily indicate lower adsorbent performance, but rather reflects the dilution of adsorbed molecules across a greater number of available surface sites [44, 45, 46]. Based on the highest removal efficiency, 3 g was identified as the optimum dosage for surfactant removal, achieving 85.91% removal with an adsorption capacity of 0.26 mg/g.

A similar dosage-dependent trend was observed for phosphate adsorption (Figure 3B). The phosphate removal efficiency increased from 45.24% at 1 g to 65.67% at 4 g. The improvement to 4 g indicates that increasing the RHA dosage provides more sites accessible for phosphate uptake. However, further increasing the dosage to 5 and 6 g reduced the removal efficiency to 63.59% and 56.92%, respectively. This reduction may be caused by particle agglomeration, overlapping adsorption sites, and a lower phosphate-to-adsorbent ratio, which limits the effective utilization of the added adsorbent mass.

The q_e value for phosphate decreased from 0.039 mg/g to 0.008 mg/g as the adsorbent dosage increased from 1 to 6 g. Although the highest adsorption capacity was obtained at the lowest dosage, the corresponding removal efficiency was relatively low. The optimum phosphate removal was achieved at 4 g, with a removal efficiency of 65.67% and an adsorption capacity of 0.014 mg/g. These results indicate that the optimum adsorbent dosage depends on the target contaminant. Surfactant removal was optimized at 3 g, whereas phosphate removal required a slightly higher dosage of 4 g, possibly due to its lower initial concentration and weaker interaction with the silica-rich RHA surface.

3.3. Effect of Contact Time

The effect of contact time on surfactant and phosphate removal by acid-activated RHA is presented in Figure 4A–B. Contact time strongly influenced the adsorption performance of both contaminants, with the highest removal efficiencies observed at 30 min. This trend indicates that the adsorption process proceeded rapidly during the early stage and reached an optimum contact time within a relatively short period.

For surfactant adsorption (Figure 4A), the removal efficiency increased from 82.59% at 15 min to 88.30% at 30 min. The adsorption capacity also increased from 0.258 mg/g to 0.276 mg/g over the same period. This rapid increase suggests that surfactant molecules were readily adsorbed onto the accessible surface sites of acid-activated RHA during the initial adsorption stage. The presence of hydroxyl- and siloxane-related functional groups on the RHA surface may contribute to surfactant uptake by providing heterogeneous surface sites for adsorption [47, 48]. Since zeta potential and pH_{pzc} analyses were not performed, the relative contributions of electrostatic interactions, hydrogen bonding, and hydrophobic association cannot be clearly separated in the present study.

After 30 min, both the removal efficiency and the adsorption capacity decreased. The surfactant removal efficiency declined to 80.12% at 45 min and 77.85% at 60 min, while q_e decreased to 0.250 and 0.243 mg/g, respectively. This decrease suggests that prolonged contact time did not improve surfactant adsorption after the optimum point. Instead, the slight reduction may be related to the reversible nature of physical adsorption, weakly bound surfactant molecules, or redistribution of adsorbed species at the solid–liquid interface. In real

laundry wastewater, this behavior may also be influenced by matrix effects because dissolved organic matter, detergent additives, and coexisting inorganic ions can compete with surfactant molecules for available adsorption sites or promote partial displacement of weakly adsorbed species [49, 50]. Therefore, the decline observed after 30 min is likely associated with a combination of adsorption–desorption equilibrium, surface rearrangement, and competitive interactions in the real wastewater matrix.

For phosphate adsorption (Figure 4B), the removal efficiency increased from 49.69% at 15 min to 66.09% at 30 min, while the adsorption capacity increased from 0.011 to 0.014 mg/g. The lower adsorption capacity of phosphate compared with that of the surfactant may be attributed to its lower initial concentration in the wastewater and to its interaction mechanism with the silica-rich RHA surface. Phosphate adsorption may be associated with hydroxyl-containing sites on the silica-rich RHA surface. However, without zeta potential, pH_{pzc}, or XPS analysis, the specific roles of electrostatic attraction, hydrogen bonding, and surface complexation remain tentative. Nevertheless, because acid-activated RHA was not impregnated with metal oxides or cationic functional groups, its affinity toward phosphate is expected to be moderate.

Beyond 30 min, phosphate removal decreased to 48.42% at 45 min and 42.20% at 60 min. The corresponding adsorption capacity also declined to 0.010 and 0.009 mg/g, respectively. This trend indicates that extending the contact time beyond 30 min may promote partial desorption or rearrangement of weakly bound phosphate species. The decrease may also be associated with competition from coexisting ions and dissolved organic matter in the real wastewater. Phosphate adsorption is sensitive to matrix composition because background organic matter and competing anions can occupy or block adsorption sites, modify surface charge interactions, or displace weakly bound phosphate from hydroxyl-containing surfaces [49, 50]. Since the present study used real laundry wastewater without matrix simplification, these competitive effects may partly explain the lower phosphate stability after the optimum contact time. Similar behavior has been observed in adsorption systems dominated by physical interactions or weak surface complexation, where equilibrium is reached rapidly, and prolonged contact does not necessarily improve removal performance [51, 52, 53, 54, 55].

Overall, the contact time results demonstrate that acid-activated RHA can remove surfactant and phosphate from real laundry wastewater within a short treatment period. A contact time of 30 min was identified as the optimum condition for both contaminants, providing the highest removal efficiencies and adsorption capacities. The reduction observed at longer contact times suggests that adsorption performance in real wastewater is affected not only by contact time but also by reversible adsorption, possible competition among wastewater constituents, and re-equilibration within the multicomponent wastewater system. Therefore, 30 min was selected as the operating contact time for subsequent adsorption analysis.

3.4. Adsorption Isotherm Analysis

The adsorption equilibrium behavior of surfactant and phosphate onto acid-activated RHA was evaluated using the Langmuir and Freundlich isotherm models. The isotherm experiments were conducted separately using single-solute surfactant and phosphate standard solutions to allow controlled variation of the initial concentration and to minimize interference from the complex real wastewater matrix during model fitting. Therefore, the isotherm analysis was intended to provide supporting insight into the individual equilibrium adsorption behavior of each contaminant, rather than to represent simultaneous adsorption in real laundry wastewater. The practical removal performance under real wastewater conditions was evaluated separately through the adsorbent dosage, contact time, and kinetic experiments. The linearized isotherm plots are presented in Figure 5, and the corresponding parameters are summarized in Table 1.

For surfactant adsorption, the Freundlich model showed an excellent correlation coefficient (R^2 = 0.9993; Figure 5B). This result indicates that surfactant adsorption onto acid-activated RHA was better represented by a heterogeneous adsorption model than by a uniform monolayer model. The Freundlich model is commonly used to describe adsorption on heterogeneous surfaces where adsorption sites have different affinities and energy distributions [36]. The Freundlich constant K_F was 0.2024 L/g, while the $1/n$ value was 2.8239. Since the $1/n$ value is greater than unity, the adsorption behavior should not be interpreted as favorable Freundlich adsorption. Instead, this value indicates non-ideal, concentration-dependent adsorption, possibly associated with low adsorption intensity, heterogeneous site distribution, and limited affinity of the non-functionalized, silica-rich RHA surface for surfactant molecules. Therefore, the Freundlich fit in this study mainly reflects surface heterogeneity rather than strong adsorption favorability.

Although the Langmuir plot for surfactant adsorption showed a high correlation coefficient (R^2 = 0.9908), the fitted line exhibited a negative slope (Figure 5A). Since the slope of the linear Langmuir equation corresponds to $1/q_{max}$, a negative slope gives a non-physical q_{max} value. Therefore, the Langmuir parameters for surfactant adsorption should not be used to infer monolayer capacity or homogeneous adsorption behavior. A high R^2 value alone is insufficient to confirm Langmuir-type adsorption when the fitted parameters are not physically meaningful. Accordingly, surfactant adsorption in this study is better interpreted using the Freundlich model.

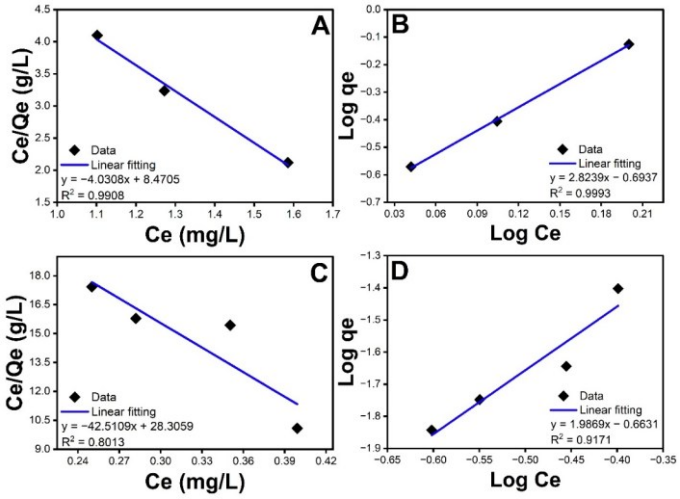

Figure 5. Linearized Langmuir and Freundlich adsorption isotherms for the adsorption of surfactant and phosphate standard solutions onto acid-activated RHA: (A) Langmuir and (B) Freundlich models for surfactant adsorption; (C) Langmuir and (D) Freundlich models for phosphate adsorption

The predominance of Freundlich-type behavior is consistent with previous reports on surfactant adsorption using biomass- and waste-derived adsorbents, where adsorption is often governed by surface heterogeneity and physical interactions rather than uniform monolayer coverage [56, 57]. Compared with engineered biochar or activated carbon systems, the adsorption capacity of acid-activated RHA is relatively low. However, this is reasonable because RHA is a simple, low-cost, non-functionalized adsorbent, and the adsorption process is mainly supported by naturally available silica-related surface groups rather than highly engineered active sites [57, 58].

For phosphate adsorption, the Freundlich model also provided a better fit than the Langmuir model, with R^2 values of 0.9171 and 0.8013, respectively (Figure 5C–D). The better agreement with the Freundlich model suggests that phosphate adsorption occurred on heterogeneous surface sites rather than through uniform monolayer coverage. The Freundlich constant K_F for phosphate was 0.2172 L/g, while the 1/*n* value was 1.9869. Similar to surfactant adsorption, a 1/*n* value greater than unity does not indicate favorable adsorption. Rather, it suggests non-ideal adsorption behavior and relatively weak adsorption intensity, which may be related to the limited availability of strong phosphate-binding sites on acid-activated RHA. This interpretation is consistent with the absence of metal oxide or cationic functionalization, which are commonly required to enhance phosphate affinity on silica-based adsorbents.

The interaction of phosphate with acid-activated RHA is likely associated with hydroxyl- and siloxane-related groups on the silica-rich surface. These groups may contribute to phosphate uptake through surface interactions with hydroxyl- and siloxane-related sites [37, 38]. Nevertheless, the exact contribution of hydrogen bonding, electrostatic interactions, and weak surface complexation cannot be distinguished from isotherm fitting alone. However, because the adsorbent was not modified with metal oxides or cationic functional groups, strong ligand-exchange or inner-sphere complexation is unlikely to dominate. This explains the relatively low adsorption capacity and the better suitability of the Freundlich model for describing phosphate adsorption. Similar Freundlich-type phosphate adsorption has been reported for heterogeneous mineral and biomass-derived adsorbents, where non-uniform adsorption energies and weak surface interactions control phosphate uptake [38].

The Langmuir plot for phosphate adsorption also showed a negative slope (Figure 5C), indicating that the Langmuir-derived q_{max} and K_L values are not physically reliable. Therefore, as with surfactant adsorption, the Langmuir model should be treated only as a comparative mathematical fitting model and not as evidence of monolayer adsorption. In contrast, adsorbents containing more reactive mineral phases or metal-based active sites often show stronger Langmuir-type phosphate adsorption because of more specific binding, ligand exchange, or precipitation mechanisms [59, 60, 61, 62]. The different behavior observed for acid-activated RHA suggests that phosphate uptake was more consistent with heterogeneous silica-based surface interactions than with highly specific chemisorption.

Overall, the isotherm analysis indicates that the adsorption of both surfactant and phosphate onto acid-activated RHA is better described by the Freundlich model. This suggests that adsorption occurs mainly on heterogeneous surface sites with non-uniform adsorption energies. The results support the role of acid-activated RHA as a low-cost adsorbent with heterogeneous silica-based surface characteristics. However, because the isotherm experiments were performed using separate standard solutions, these findings should be interpreted as controlled equilibrium evidence for individual pollutant adsorption, while the practical removal performance in real laundry wastewater is discussed based on the dosage, contact time, and kinetic experiments.

Table 1. Adsorption isotherm parameters for surfactant and phosphate adsorption from single-solute standard solutions

Adsorption isotherm parameter	Unit	Surfactant Langmuir	Surfactant Freundlich	Phosphate Langmuir	Phosphate Freundlich
q_{max}	mg/g	N.A.	-	N.A.	-
K_L	L/mg	N.A.	-	N.A.	-
K_f	L/g	-	0.2024	-	0.2172
$1/n$	-	-	2.8239	-	1.9869
n	-	-	0.3541	-	0.5032
R^2	-	0.9908	0.9993	0.8013	0.9171

N.A.: not applicable because the Langmuir linear fitting produced a negative slope, resulting in non-physical Langmuir parameters.

3.5. Kinetic Adsorption Behavior

The kinetic adsorption behavior of surfactant and phosphate from real laundry wastewater onto sulfuric acid–activated RHA is presented in Figure 6 and summarized in Table 2. Both contaminants showed rapid uptake during the initial adsorption period, followed by an apparent equilibrium within approximately 30 min. This rapid adsorption behavior suggests that a substantial fraction of accessible surface sites was occupied during the early stage of contact between the adsorbent and wastewater. Such fast uptake is advantageous for practical wastewater treatment because it indicates that contaminant removal can be achieved within a relatively short contact time. Similar rapid adsorption behavior has been reported for biomass- and ash-derived adsorbents, including fly ash and rice husk–based materials [63, 64].

For surfactant adsorption, the pseudo-first-order model provided a good fit to the experimental data, with an R^2 value of 0.988. The fitted equilibrium adsorption capacity was 0.257 mg/g, which was close to the experimental adsorption capacity observed near equilibrium. This agreement indicates that the pseudo-first-order model can reasonably describe time-dependent surfactant uptake under the conditions studied. However, the very high k_1 value reflects rapid initial adsorption and should be interpreted with caution, as fast equilibrium and limited kinetic data points can reduce the reliability of rate constant estimates.

The pseudo-second-order model also produced a high correlation coefficient for surfactant adsorption (R^2 = 0.988); however, the fitted k_2 value was negative. Since a negative adsorption rate constant is not physically meaningful, the pseudo-second-order model cannot be considered valid for describing surfactant adsorption in this system. Therefore, the pseudo-second-order result for surfactant should be treated only as a mathematical fit and should not be used to infer chemisorption or rate-controlling mechanisms. This also indicates that model selection should not be based solely on R^2, but must also consider the physical meaning of the fitted parameters.

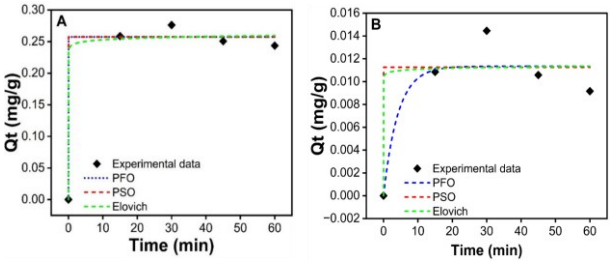

Figure 6. Kinetic adsorption behavior of (A) surfactant and (B) phosphate from real laundry wastewater onto sulfuric acid–activated RHA

For phosphate adsorption, the pseudo-first-order and pseudo-second-order models produced lower correlation coefficients, with R^2 values of 0.871 and 0.870, respectively. These values indicate that neither model fully captured the phosphate adsorption behavior under the experimental conditions. The relatively low adsorption capacity may be associated with the low initial phosphate concentration in real laundry wastewater and the limited availability of strong phosphate-binding sites on the silica-rich RHA surface. Unlike metal-modified adsorbents, acid-activated RHA lacks highly reactive metal centers for phosphate binding; therefore, phosphate uptake is expected to occur mainly through weaker interactions with hydroxyl- and siloxane-related surface groups.

Among the tested models, the Elovich model provided the highest correlation coefficients for both surfactant and phosphate adsorption, with R^2 values of 0.999. This result suggests that adsorption occurred on energetically heterogeneous surface sites, where the adsorption rate decreased progressively as surface coverage increased. Such behavior is consistent with the heterogeneous surface morphology of acid-activated RHA observed in the SEM images and with the presence of silanol and siloxane groups indicated by FTIR analysis. However, because the adsorption process reached equilibrium rapidly and the kinetic dataset contained a limited number of time points, the Elovich fitting should be interpreted as supporting evidence of surface heterogeneity rather than definitive proof of a specific adsorption mechanism.

Table 2. Adsorption kinetic parameters for surfactant and phosphate removal from real laundry wastewater using sulfuric acid–activated RHA

Kinetic model	Parameter	Unit	Surfactant	Phosphate
Pseudo-first-order $q_t = q_e\,(1 - e^{-k_1 t})$	q_t	mg/g	0.257	0.0113
	k_1	min^{-1}	4929.061	0.238
	R^2	-	0.988	0.871
Pseudo-second-order $q_t = \frac{k_2\, q_e^2\, t}{1 + k_2\, q_e\, t}$	q_t	mg/g	0.257	0.0112
	k_2	g mg^{-1} min^{-1}	N.A.	1.884
	R^2	-	0.988	0.87
Elovich $q_t = \frac{1}{\beta} ln\,(1 + \alpha\beta t)$	α	mg g^{-1} min^{-1}	2.306	4.36
	β	g/mg	271.36	6748.538
	R^2	-	0.999	0.999

N.A.: not applicable because the pseudo-second-order fitting produced a negative k_2 value for surfactant adsorption, which is not physically meaningful. q_e, equilibrium adsorption capacity (mg/g) at t; k_1, pseudo-first-order rate constant (min^{-1}); k_2, pseudo-second-order rate constant (g mg^{-1} min^{-1}); α, initial adsorption rate constant of Elovich model (mg g^{-1} min^{-1}); β, desorption constant related to surface coverage and activation energy (g/mg); R^2, correlation coefficient.

Overall, the kinetic analysis indicates that acid-activated RHA can rapidly remove surfactant and phosphate from real laundry wastewater, with an optimum contact time of approximately 30 min. The kinetic fitting suggests that the adsorption process is better represented by models that account for rapid uptake and surface heterogeneity, particularly the Elovich model. Nevertheless, the kinetic parameters should be interpreted cautiously, especially for models producing non-physical values, such as the negative k_2 obtained for surfactant adsorption. Therefore, kinetic modeling in this study is best used to support the observed rapid removal behavior and heterogeneous adsorption tendency, rather than to assign a definitive rate-controlling mechanism.

3.6. FTIR Analysis of Adsorbent After Adsorption

The FTIR spectra of acid-activated RHA before and after adsorption are presented in Figure 7. Spectrum A represents acid-activated RHA, while spectra B and C represent RHA after surfactant and phosphate adsorption, respectively. Changes in band intensity and spectral features after adsorption suggest the involvement of surface functional groups during contaminant uptake. These variations indicate that surfactant and phosphate interact with the silica-rich surface of acid-activated RHA. However, the interactions should be interpreted cautiously because several characteristic bands may overlap within the same wavenumber regions.

A broad absorption band centered at approximately 3450 cm^{-1} was observed in all spectra. This band is commonly attributed to the stretching vibration of hydroxyl groups associated with surface silanol groups (Si–OH) and adsorbed water molecules. After surfactant adsorption, the intensity of this band increased and became broader, suggesting changes in the hydroxyl-related environment after adsorption. This change may be associated with surface interactions between surfactant molecules and hydroxyl-containing groups, although FTIR alone cannot confirm the specific type of interaction. A similar broad band was observed after phosphate adsorption, indicating that hydroxyl-related groups also contributed to phosphate uptake. These observations are consistent with the presence of silanol groups on silica-based materials and their role as potential interaction sites for polar adsorbates [65, 66].

For surfactant-loaded RHA, changes were observed around 1636 cm^{-1}. This band may be associated with the bending vibration of adsorbed water and/or the contribution of organic functional groups from surfactant species, including aromatic C=C vibrations from linear alkylbenzene sulfonate-type surfactants [67]. The increased intensity of this band after surfactant adsorption suggests that surfactant molecules were retained on the RHA surface. However, no distinct new bands indicating covalent bond formation were observed. Therefore, surfactant adsorption is more cautiously interpreted as being associated with weak physical surface interactions between surfactant moieties and the silica-rich RHA surface [68]. The possible involvement of hydrogen bonding, van der Waals forces, dipole interactions, and hydrophobic association remains tentative without additional surface-sensitive characterization. This interpretation is consistent with the Freundlich-dominated adsorption behavior, which suggests adsorption on heterogeneous surface sites.

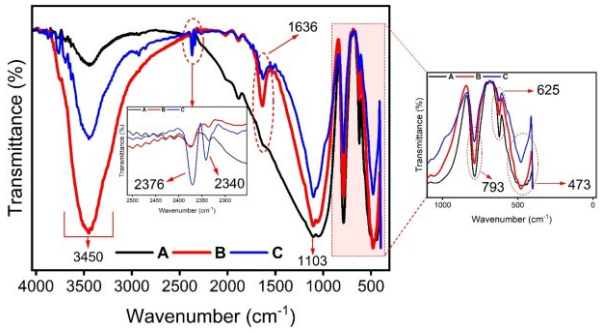

Figure 7. FTIR spectra of RHA-based adsorbent: (A) after H_2SO_4 activation, (B) after surfactant adsorption, and (C) after phosphate adsorption

After phosphate adsorption, noticeable changes were observed in the fingerprint region, particularly around the strong Si–O stretching band near 1103 cm^{-1}. The decrease or modification of this band suggests that siloxane and silanol-related groups were involved in phosphate adsorption [69]. Because phosphate vibrational bands can overlap with the strong Si–O stretching region of silica-based materials, the absence of clearly separated phosphate-specific peaks does not necessarily indicate the absence of phosphate adsorption. Instead, the spectral changes suggest that phosphate uptake may involve interactions with surface hydroxyl and siloxane-related groups. However, the possible roles of hydrogen bonding, electrostatic attraction, and weak surface complexation should be regarded as proposed interactions rather than confirmed mechanisms.

Additional spectral variations were observed in the lower wavenumber region between 700 and 400 cm^{-1}, particularly near 793, 625, and 473 cm^{-1}. The band near 793 cm^{-1} is generally associated with symmetric Si–O–Si vibrations, while bands around 625 and 473 cm^{-1} may be related to Si–O bending and rocking modes [69, 70]. The changes in intensity in this region after surfactant and phosphate adsorption indicate that the local silica network environment was affected by surface interactions with the adsorbed species. However, these changes did not indicate a major structural disruption of the RHA framework, consistent with XRD results showing that the main silica-related diffraction features were retained after acid activation.

Overall, the FTIR results support the involvement of hydroxyl, silanol, siloxane, and silica-related surface groups in the adsorption of surfactant and phosphate onto acid-activated RHA. However, these results should be interpreted as supportive evidence of surface involvement rather than definitive mechanistic proof. Distinguishing the relative contributions of hydrogen bonding, electrostatic interactions, surface complexation, and hydrophobic association would require additional analyses such as zeta potential, pH_{pzc}, XPS, or surface charge measurements.

4. Conclusion

This study demonstrates the potential of sulfuric acid–activated rice husk ash (RHA) as a low-cost adsorbent for removing surfactants and phosphates from real laundry wastewater. Acid activation modified the observable characteristics of RHA while preserving its silica-based framework, producing a rougher morphology and retaining hydroxyl- and siloxane-related functional groups. Batch adsorption experiments showed that the optimum dosage was 3 g for surfactant removal and 4 g for phosphate removal, with an optimum contact time of 30 min for both contaminants. Controlled isotherm experiments using separate single-solute standard solutions indicated that adsorption was better described by the Freundlich model, suggesting heterogeneous surface interactions. Kinetic analysis using real laundry wastewater showed rapid uptake, with the Elovich model providing the best overall fit. These findings suggest that acid-activated RHA is a promising, simple, and affordable adsorbent for treating laundry wastewater. However, further studies on regeneration, reusability, column performance, and cost analysis are needed to support long-term practical application.

References

[1] Valeria Mezzanotte, Sara Venturelli, Riccardo Paoli, Elena Collina, Francesco Romagnoli, Life Cycle Assessment of an industrial laundry: A case study in the Italian context, *Cleaner Environmental Systems*, 16, (2025), 100246 https://doi.org/10.1016/j.cesys.2024.100246

[2] Joko Sutrisno, Muhammad Al Kholif, Linda Purwanti, Indah Nurhayati, Bibliometrics Analysis and Future Study Trends in Anaerobic Biofilter Systems for Laundry Wastewater Treatment, *International Journal of Marine Engineering Innovation and Research*, 9, 3, (2024), 486-494 https://doi.org/10.12962/j25481479.v9i3.21544

[3] Sushil Kumar, Ali Khosravanipour Mostafazadeh, Patrick Drogui, R. D. Tyagi, Treatment of laundry wastewater using extracellular polymeric substances (EPS), *Environmental Systems Research*, 12, (2023), 10 https://doi.org/10.1186/s40068-023-00289-5

[4] Elisenda Pulido Melián, Dunia E. Santiago, Elena León, Jenifer Vaswani Reboso, José Alberto Herrera-Melián, Treatment of laundry wastewater by different processes: Optimization and life cycle assessment, *Journal of Environmental Chemical Engineering*, 11, 2, (2023), 109302 https://doi.org/10.1016/j.jece.2023.109302

[5] Kah Chun Ho, Yeit Haan Teow, Jing Yao Sum, Zhe Jia Ng, Abdul Wahab Mohammad, Water pathways through the ages: Integrated laundry wastewater treatment for pollution prevention, *Science of The Total Environment*, 760, (2021), 143966 https://doi.org/10.1016/j.scitotenv.2020.143966

[6] Suaibu O. Badmus, Hussein K. Amusa, Tajudeen A. Oyehan, Tawfik A. Saleh, Environmental Risks and Toxicity of Surfactants: Overview of Analysis, Assessment, and Remediation Techniques, *Environmental Science and Pollution Research*, 28, (2021), 62085-62104 https://doi.org/10.1007/s11356-021-16483-w

[7] Roberta Frinhani Nunes, Antonio Carlos Silva Costa Teixeira, An overview on surfactants as pollutants of concern: Occurrence, impacts and persulfate-based remediation technologies, *Chemosphere*, 300, (2022), 134507 https://doi.org/10.1016/j.chemosphere.2022.134507

[8] J. Lan, P. Liu, X. Hu, S. Zhu, Harmful Algal Blooms in Eutrophic Marine Environments: Causes, Monitoring, and Treatment, *Water*, 16, (2024), 2525 https://doi.org/10.3390/w16172525

[9] Fernando García-Ávila, Estefanía García-Pizarro, Gabriela Malla-Aguilar, Camila Sánchez-Cabrera, Manuel Cadme-Galabay, Lorgio Valdiviezo-Gonzales, Rita Cabello-Torres, Influence of Nutrients on Aquatic Vegetation and Trophic Status of Lakes: Analysis of Eutrophication and Mitigation, *Results in Engineering*, 27, (2025), 106381 https://doi.org/10.1016/j.rineng.2025.106381

[10] Sugito Sugito, Aliffia Rica Ambima, Muhammad Al Kholif, Firda Lutfiatul Fitria, Optimizing Laundry

Wastewater Treatment: A Hybrid Approach Using Poly-Aluminum Chloride Coagulation and Activated Carbon Adsorption, *International Journal of Marine Engineering Innovation and Research*, 10, 1, (2025), 146-154 https://doi.org/10.12962/j25481479.v10i1

[11] Derrick Dadebo, Mona G. Ibrahim, Manabu Fujii, Mahmoud Nasr, Sequential Treatment of Surfactant-Laden Wastewater Using Low-Cost Rice Husk Ash Coagulant and Activated Carbon: Modeling, Optimization, Characterization, and Techno-Economic Analysis, *Bioresource Technology Reports*, 22, (2023), 101464 https://doi.org/10.1016/j.biteb.2023.101464

[12] Jiahao Luo, Xin Jin, Yadong Wang, Pengkang Jin, Advanced Treatment of Laundry Wastewater by Electro-Hybrid Ozonation–Coagulation Process: Surfactant and Microplastic Removal and Mechanism, *Water*, 14, 24, (2022), 4138 https://doi.org/10.3390/w14244138

[13] A. Saravanan, V. C. Deivayanai, P. Senthil Kumar, Gayathri Rangasamy, R. V. Hemavathy, T. Harshana, N. Gayathri, Krishnapandi Alagumalai, A detailed review on advanced oxidation process in treatment of wastewater: Mechanism, challenges and future outlook, *Chemosphere*, 308, (2022), 136524 https://doi.org/10.1016/j.chemosphere.2022.136524

[14] Nafiu Umar Barambu, Derrick Peter, Mohd Hizami Mohd Yusoff, Muhammad Roil Bilad, Norazanita Shamsuddin, Lisendra Marbelia, Nik Abdul Hadi Nordin, Juhana Jaafar, Detergent and Water Recovery from Laundry Wastewater Using Tilted Panel Membrane Filtration System, *Membranes*, 10, 10, (2020), 260 https://doi.org/10.3390/membranes10100260

[15] Terelle Ramcharan, Ajay Bissessur, Treatment of laundry wastewater by biological and electrocoagulation methods, *Water Science and Technology*, 75, 1, (2017), 84-93 https://doi.org/10.2166/wst.2016.464

[16] Harmin Sulistiyaning Titah, Felicia Naila Nasir, The Use of Granular Activated Carbon and Zeolite as an Adsorbent to Reduce the Concentration of Phosphate, Chemical Oxygen Demand and Total Suspended Solid in Laundry Wastewater, *Journal of Ecological Engineering*, 25, 4, (2024), 170-183 https://doi.org/10.12911/22998993/184089

[17] Andriy Anta Kacaribu, Yuliani Aisyah, Febriani, Darwin, Development of wastewater treatment methods for palm oil mill effluent (POME): A comprehensive review, *Resources, Chemicals and Materials*, 4, 4, (2025), 100130 https://doi.org/10.1016/j.recm.2025.100130

[18] Julinawati Julinawati, Rahmi Rahmi, Zuhrah Putri Karnain, Irfan Mustafa, Kartika M. Z., Mutia Farida, Andriy Anta Kacaribu, Preparation of magnetic-activated biocarbon composite from Red Algae for dye removal from water, *Journal of Ecological Engineering*, 26, 8, (2025), 67-85 https://doi.org/10.12911/22998993/203746

[19] Rahmi, Melsi Agustia Zulasma, Lelifajri, Andriy Anta Kacaribu, Preparation of Chitosan-Glycidyl Methacrylate Grafted Rice Straw Cellulose (Chi/GMAgCell) Composite Film for Cadmium Ions Removal from Water, *International Journal of Design and Nature and Ecodynamics*, 20, 3, (2025), 515-522 https://doi.org/10.18280/ijdne.200306

[20] Andriy Anta Kacaribu, Yuliani Aisyah, Febriani Febriani, Darwin Darwin, The Development of Green Polylactic Acid (PLA) Composites for the Wastewater Treatment Process – A Review, *Engineering Transactions*, 73, 3, (2025), 485-524 https://doi.org/10.24423/engtrans.3534.2025

[21] Andriy Anta Kacaribu, Darwin Darwin, Biotechnological Lactic Acid Production from Low-Cost Renewable Sources via Anaerobic Microbial Processes, *BioTechnologia*, 105, 2, (2024), 179-194 https://doi.org/10.5114/bta.2024.139757

[22] Ching Yin Ng, Ying Ying Tan, Amelia Chiang Kar Mun, Law Yong Ng, Comparison study of adsorbent produced from renewable resources: Oil palm empty fruit bunch and rice husk, *Materials Today: Proceedings*, 29, (2020), 149-155 https://doi.org/10.1016/j.matpr.2020.05.642

[23] José Lugo-Arias, Julia González-Álvarez, Aymer Maturana, José Villa-Parejo, Carlos Barraza-Heras, Removal of nitrate and phosphate from aqueous solutions using bioadsorbents derived from agro-industrial wastes of rice husk and corn stalk, *Biomass Conversion and Biorefinery*, 15, (2025), 19453-19475 https://doi.org/10.1007/s13399-025-06720-4

[24] Shaswat Kumar Das, Adeolu Adediran, Cyriaque Rodrigue Kaze, Syed Mohammed Mustakim, Nordine Leklou, Production, characteristics, and utilization of rice husk ash in alkali activated materials: An overview of fresh and hardened state properties, *Construction and Building Materials*, 345, (2022), 128341 https://doi.org/10.1016/j.conbuildmat.2022.128341

[25] Hadid Sukmana, Milivoj Radojčin, Tamás Gyulavári, Gábor Kozma, Zoltán Kónya, Cecilia Hodúr, Utilization of rice husks as effective bioadsorbents for methylene blue removal from wastewater: characterization, adsorption performance, and regeneration studies, *Applied Water Science*, 15, (2025), 148 https://doi.org/10.1007/s13201-025-02511-4

[26] Ben McLean, Irene Yarovsky, Structure, Properties, and Applications of Silica Nanoparticles: Recent Theoretical Modeling Advances, Challenges, and Future Directions, *Small*, 20, (2024), 2405299 https://doi.org/10.1002/smll.202405299

[27] A. Hosseinnia, M. S. Hashtroudi, M. Pazouki, M. Banifatemi, Removal of Surfactants from Wastewater by Rice Husk, *Iranian Journal of Chemical Engineering*, 3, 3, (2006), 44-50

[28] Phuoc Toan Phan, Trung Thanh Nguyen, Surapol Padungthon, Thuy Nguyen Thi, Nguyen Nhat Huy, A Novel Conjugate Mechanism for Enhancing the Adsorption Capacity of Amine-Functionalized Activated Rice Husk Ash for Simultaneous Removal of Organics and Anions in Wastewater: Experimental and Theoretical Explanations, *ACS Omega*, 7, 33, (2022), 28866-28874 https://doi.org/10.1021/acsomega.2c01955

[29] Nur Diyana Suzaimi, Pei Sean Goh, Nik Ahmad Nizam Nik Malek, Jun Wei Lim, Ahmad Fauzi Ismail, Enhancing the performance of porous rice husk silica through branched polyethyleneimine grafting for phosphate adsorption, *Arabian Journal of Chemistry*, 13, 8, (2020), 6682-6695 https://doi.org/10.1016/j.arabjc.2020.06.023

[30] American Public Health Association (APHA), *Standard Methods for the Examination of Water and Wastewater*, 22nd ed., Washington, DC, 2012,

[31] P. U. Nzereogu, A. D. Omah, F. I. Ezema, E. I. Iwuoha, A. C. Nwanya, Silica extraction from rice husk: Comprehensive review and applications, *Hybrid Advances*, 4, (2023), 100111 https://doi.org/10.1016/j.hybadv.2023.100111

[32] Ruth H. Ellerbrock, Mathias Stein, Jörg Schaller, Comparing silicon mineral species of different crystallinity using Fourier transform infrared spectroscopy, *Frontiers in Environmental Chemistry*, 5, (2024), 1462678 https://doi.org/10.3389/fenvc.2024.1462678

[33] Rohani Abu Bakar, Rosiyah Yahya, Seng Neon Gan, Production of High Purity Amorphous Silica from Rice Husk, *Procedia Chemistry*, 19, (2016), 189-195 https://doi.org/10.1016/j.proche.2016.03.092

[34] Mai-Mari Hirose Carlsen, Yukie Saito, Phase Diagram of SiO_2 Crystallization upon Rice Husk Combustion to Control Silica Ash Quality, *Waste Management*, 182, (2024), 55-62 https://doi.org/10.1016/j.wasman.2024.04.009

[35] P. C. Nwadibia, J. C. Eze, D. I. Anyaogu, H. O. Abugu, P. M. Ejikeme, Adsorptive capacity of activated carbon derived from rice husks for azo dye removal from solution, *Discover Chemistry*, 2, (2025), 152 https://doi.org/10.1007/s44371-025-00233-9

[36] Shams Kalam, Sidqi A. Abu-Khamsin, Muhammad Shahzad Kamal, Shirish Patil, Surfactant Adsorption Isotherms: A Review, *ACS Omega*, 6, 48, (2021), 32342-32348 https://doi.org/10.1021/acsomega.1c04661

[37] Dimitrios A. Giannakoudakis, Yongchang Sun, Wastewater Treatments Based on Adsorption, Catalysis, Biodegradation, and Beyond, *Molecules*, 29, 22, (2024), 5470 https://doi.org/10.3390/molecules29225470

[38] Prangya Ranjan Rout, Puspendu Bhunia, Rajesh Roshan Dash, Modeling isotherms, kinetics and understanding the mechanism of phosphate adsorption onto a solid waste: Ground burnt patties, *Journal of Environmental Chemical Engineering*, 2, 3, (2014), 1331-1342 https://doi.org/10.1016/j.jece.2014.04.017

[39] Joshua O. Ighalo, Eduardo Alberto López-Maldonado, Chinenye Adaobi Igwegbe, Juan Ramón López López, Perla Fabiola Méndez Herrera, Titus Chinedu Egbosiuba, Etinosa Osaro, Kanika Dulta, Panagiotis Haskis, Dionysios Koulougliotis, Ioannis Anastopoulos, A comprehensive review of the adsorption of Eriochrome Black T (EBT) from aqueous solutions, *Sustainable Chemistry for the Environment*, 12, (2025), 100299 https://doi.org/10.1016/j.scenv.2025.100299

[40] Oluseyi S. Salami, Masixole Sihlahla, Bongumusa S. Dladla, Nomvano Mketo, Adsorptive removal of additive potent organic toxicants from beverages and contaminated waters: A critical review of adsorbent materials, kinetics, isotherms, thermodynamics, mechanisms, and future prospects, *Separation and Purification Technology*, 380, (2026), 135453 https://doi.org/10.1016/j.seppur.2025.135453

[41] Weigao Zhao, Chenjie Hao, Yiping Guo, Wanfei Shao, Yimei Tian, Peng Zhao, Optimization of Adsorption Conditions Using Response Surface Methodology for Tetracycline Removal by $MnFe_2O_4$/Multi-Wall Carbon Nanotubes, *Water*, 15, 13, (2023), 2392 https://doi.org/10.3390/w15132392

[42] K. A. Adegoke, S. O. Akinnawo, T. A. Adebusuyi, O. A. Ajala, R. O. Adegoke, N. W. Maxakato, O. S. Bello, Modified biomass adsorbents for removal of organic pollutants: a review of batch and optimization studies, *International Journal of Environmental Science and Technology*, 20, (2023), 11615-11644 https://doi.org/10.1007/s13762-023-04872-2

[43] Julinawati Julinawati, Eka Nadia, Irfan Mustafa, Suryati Suryati, Preparation and Characterization of Cellulose-Clay Composite Using Indonesian Natural Bentonite for Cr(VI) Adsorption, *Journal of Multidisciplinary Applied Natural Science*, 5, 3, (2025), 884-896 https://doi.org/10.47352/jmans.2774-3047.289

[44] Riana Ayu Kusumadewi, Firdaus Ali, Sucipta Laksono, Nandy Putra, Andhy M. Fathoni, Khairu Rezqi, Teuku Meurah Indra Mahlia, Organic Adsorbents for Removing Dissolved Organic Matter (DOM): Toward Low-Cost Water Purification, *Water*, 17, 16, (2025), 2433 https://doi.org/10.3390/w17162433

[45] Huda Alkhaldi, Sarah Alharthi, Salha Alharthi, Hind A. AlGhamdi, Yasmeen M. AlZahrani, Safwat A. Mahmoud, Lamia Galal Amin, Nora Hamad Al-Shaalan, Waleed E. Boraie, Mohamed S. Attia, Samera Ali Al-Gahtany, Nadiah Aldaleeli, Mohamed Mohamady Ghobashy, A. I. Sharshir, Mohamed Madani, Reem Darwesh, Sana F. Abaza, Sustainable Polymeric Adsorbents for Adsorption-Based Water Remediation and Pathogen Deactivation: A Review, *RSC Advances*, 14, 45, (2024), 33143-33190 https://doi.org/10.1039/D4RA05269B

[46] Imene Gritli, Hajer Chemingui, Kais Djebali, Walid Mabrouk, Amor Hafiane, Riadh Marzouki, Salah Ammar, Radhouane Chtourou, Sherif M. A. S. Keshk, Methylene Blue Adsorption by Fe_3O_4 Nanoparticles: An Optimization Study Using Response Surface Methodology, *Chemical Engineering and Technology*, 47, 10, (2024), e202400006 https://doi.org/10.1002/ceat.202400006

[47] Ahmed I. Osman, Eman M. Abd El-Monaem, Ahmed M. Elgarahy, Chukwunonso O. Aniagor, Mohamed Hosny, Mohamed Farghali, Emanne Rashad, Marcel I. Ejimofor, Eduardo A. López-Maldonado, Ikko Ihara, Pow-Seng Yap, David W. Rooney, Abdelazeem S. Eltaweil, Methods to prepare biosorbents and magnetic sorbents for water treatment: a review, *Environmental Chemistry Letters*, 21, (2023), 2337-2398 https://doi.org/10.1007/s10311-023-01603-4

[48] Janaína Oliveira Gonçalves, André Rodríguez Leones, Bruna Silva de Farias, Mariele Dalmolin da Silva, Débora Pez Jaeschke, Sibele Santos Fernandes, Anelise Christ Ribeiro, Tito Roberto Santanna Cadaval Jr., Luiz Antonio de Almeida Pinto, A Comprehensive Review of Agricultural Residue-Derived Bioadsorbents for Emerging Contaminant Removal, *Water*, 17, 14, (2025), 2141 https://doi.org/10.3390/w17142141

[49] Geert Aschermann, Corinna Schröder, Frederik Zietzschmann, Martin Jekel, Organic micropollutant desorption in various water matrices - Activated

carbon pore characteristics determine the reversibility of adsorption, *Chemosphere*, 237, (2019), 124415 https://doi.org/10.1016/j.chemosphere.2019.124415

[50] Liping Weng, Flora Alonso Vega, Willem H. Van Riemsdijk, Competitive and Synergistic Effects in pH Dependent Phosphate Adsorption in Soils: LCD Modeling, *Environmental Science and Technology*, 45, 19, (2011), 8420-8428 https://doi.org/10.1021/es201844d

[51] Hadjer Bousemat, Samira Ziane-Hezil, Saadiya Benatmane, Fatiha Bessaha, Gania Bessaha, Ali Çoruh, Mika Sillanpää, Moonis Ali Khan, Experimental and modeling studies for the simultaneous removal anionic dyes in single and binary systems using activated clay, *Scientific Reports*, 15, (2025), 45512 https://doi.org/10.1038/s41598-025-30039-9

[52] Despina A. Gkika, Athanasia K. Tolkou, Ioannis A. Katsoyiannis, George Z. Kyzas, The adsorption-desorption-regeneration pathway to a circular economy: The role of waste-derived adsorbents on chromium removal, *Separation and Purification Technology*, 368, (2025), 132996 https://doi.org/10.1016/j.seppur.2025.132996

[53] Chenhao Sun, Zhongyang Luo, Peng Yu, Qinhui Wang, Comparative Study on the Performance and Mechanism of Adsorption–Oriented Phosphorus–Modified High–Efficiency and Durable Activated Biochar from Fast Pyrolysis, *Energies*, 16, 14, (2023), 5363 https://doi.org/10.3390/en16145363

[54] Yanqiao Dong, Junfang Liu, Adsorption and Solidification/Stabilization of Phenol by Slag-Based Geopolymer-Biochar Composite, *Desalination and Water Treatment*, 323, (2025), 101327 https://doi.org/10.1016/j.dwt.2025.101327

[55] Julinawati Julinawati, Febriani Febriani, Irfan Mustafa, Fathurrahmi Fathurrahmi, Rahmi Rahmi, Sheilatina Sheilatina, Khairunnas Ahmad, Kana Puspita, Muhammad Iqhrammullah, Tryptophan-Based Organoclay for Aqueous Naphthol Blue Black Removal: Preparation, Characterization, and Batch Adsorption Studies, *Journal of Ecological Engineering*, 24, 7, (2023), 274-284 https://doi.org/10.12911/22998993/165781

[56] N. S. Ersa, M. F. Ikhwali, T. U. Karunia, Adsorption mechanism on surfactant removal using eggshell waste and rice straw as economically biosorbent, *IOP Conference Series: Earth and Environmental Science*, 871, 1, (2021), 012034 http://doi.org/10.1088/1755-1315/871/1/012034

[57] J. I. Bautista Quispe, L. C. Campos, O. Mašek, A. Bogush, Removal of anionic surfactant from aqueous solutions by adsorption onto biochars: characterisation, kinetics, and mechanism, *Environmental Technology*, 45, 26, (2024), 5723-5744 https://doi.org/10.1080/09593330.2024.2304677

[58] Thaiara Ramires dos Reis, Donizeti Leonardo Mancini Tolari, Ana Claudia Pedrozo da Silva, Elton Guntendorfer Bonafé, Rafael Block Samulewski, André Luiz Tessaro, Use of Domestic Polymeric Waste for Surfactant Removal from Wastewater, *Sustainable Chemistry*, 6, 1, (2025), 6 https://doi.org/10.3390/suschem6010006

[59] Uduakobong A. Edet, Augustine O. Ifelebuegu, Kinetics, Isotherms, and Thermodynamic Modeling of the Adsorption of Phosphates from Model Wastewater Using Recycled Brick Waste, *Processes*, 8, 6, (2020), 665 https://doi.org/10.3390/pr8060665

[60] Noorul Hudai Abdullah, Nur Amirah Adnan, Nur Fatin Nadiah Mohd Rashidi, Mohamad Syahrul Syazwan Yaacob, Nur Atikah Abdul Salim, Comparing the adsorption isotherms and kinetics of phosphate adsorption on various waste shells as adsorbent, *Water Practice and Technology*, 17, 5, (2022), 974-985 http://doi.org/10.2166/wpt.2022.051

[61] Inga Hilbrandt, Vito Lehmann, Frederik Zietzschmann, Aki Sebastian Ruhl, Martin Jekel, Quantification and isotherm modelling of competitive phosphate and silicate adsorption onto micro-sized granular ferric hydroxide, *RSC Advances*, 9, 41, (2019), 23642-23651 http://doi.org/10.1039/c9ra04865k

[62] Veranica, Aster Rahayu, Maryudi, Hakika Dhias Cahya, Lim Lee Wah, Anggresani Lia, Isotherm Adsorption of Ion Phosphate from Vinasse Waste Using Quaternary Ammonium Polymer as Adsorbent in Term Effect of Temperature, *Sains Natural: Journal of Biology and Chemistry*, 14, 2, (2024), 91-97 http://doi.org/10.31938/jsn.v14i2.720

[63] Ahmer Ali Siyal, Rashid Shamsuddin, Aaron Low, Arif Hidayat, Adsorption Kinetics, Isotherms, and Thermodynamics of Removal of Anionic Surfactant from Aqueous Solution Using Fly Ash, *Water, Air, & Soil Pollution*, 231, 10, (2020), 509 https://doi.org/10.1007/s11270-020-04879-2

[64] Moaaz K. Seliem, Sridhar Komarneni, Mostafa R. Abu Khadra, Phosphate removal from solution by composite of MCM-41 silica with rice husk: Kinetic and equilibrium studies, *Microporous and Mesoporous Materials*, 224, (2016), 51-57 https://doi.org/10.1016/j.micromeso.2015.11.011

[65] Marialore Sulpizi, Marie-Pierre Gaigeot, Michiel Sprik, The Silica–Water Interface: How the Silanols Determine the Surface Acidity and Modulate the Water Properties, *Journal of Chemical Theory and Computation*, 8, 3, (2012), 1037-1047 http://doi.org/10.1021/ct2007154

[66] Svetlana A. Kozlova, Sergey D. Kirik, Post-Synthetic Activation of Silanol Covering in the Mesostructured Silicate Materials MCM-41 and SBA-15, *Microporous and Mesoporous Materials*, 133, 1-3, (2010), 124-133 https://doi.org/10.1016/j.micromeso.2010.04.024

[67] Adél Anna Ádám, Szilveszter Ziegenheim, László Janovák, Márton Szabados, Csaba Bús, Ákos Kukovecz, Zoltán Kónya, Imre Dékány, Pál Sipos, Bence Kutus, Binding of Ca^{2+} Ions to Alkylbenzene Sulfonates: Micelle Formation, Second Critical Concentration and Precipitation, *Materials*, 16, 2, (2023), 494 https://doi.org/10.3390/ma16020494

[68] Shui Cheung Edgar Leung, Dushanthi Wanninayake, Dechao Chen, Nam-Trung Nguyen, Qin Li, Physicochemical properties and interactions of perfluoroalkyl substances (PFAS) - Challenges and opportunities in sensing and remediation, *Science of The Total Environment*, 905, (2023), 166764 https://doi.org/10.1016/j.scitotenv.2023.166764

[69] Nuryono Nuryono, Sukamto Sukamto, Eko Sri Kunarti, Philip Anggo Krisbiantoro, Wan Nazwanie Wan Abdullah, Yuichi Kamiya, Magnetically separable silica-chitosan hybrids for efficient phosphate adsorption in aqueous solution, *Case Studies in Chemical and Environmental Engineering*, 11, (2025), 101100 https://doi.org/10.1016/j.cscee.2025.101100

[70] Midhun C. D. Dominic, P. M. Sabura Begum, Rani Joseph, Daisy Joseph, Prabith Kumar, Ayswarya E. P., Synthesis, Characterization and Application of Rice Husk Nanosilica in Natural Rubber, *International Journal of Science, Environmental Technology*, 2, 5, (2013), 1027–1035